Journal of Hazardous Materials 221–222 (2012) 288–297

Contents lists available at SciVerse ScienceDirect

Journal of Hazardous Materials

journal homepage: www.elsevier.com/locate/jhazmat

# Optimization of the electro-Fenton and solar photoelectro-Fenton treatments of sulfanilic acid solutions using a pre-pilot flow plant by response surface methodology

Abdellatif El-Ghenymy[a,b], Sergi Garcia-Segura[a], Rosa María Rodríguez[a], Enric Brillas[a,*], Mohamed Soussi El Begrani[b], Ben Ali Abdelouahid[b]

[a] Laboratori d'Electroquímica dels Materials i del Medi Ambient, Departament de Química Física, Facultat de Química, Universitat de Barcelona, Martí i Franquès 1-11, 08028 Barcelona, Spain

[b] Département de Chimie, Faculté des Sciences, Université Abdelmalek Essaâdi, M'Hannech II B.P.2121, C.P. 93002 Tétouan, Morocco

ARTICLE INFO

*Article history:*
Received 2 February 2012
Received in revised form 18 April 2012
Accepted 22 April 2012
Available online 28 April 2012

*Keywords:*
Central composite rotatable design
Electro-Fenton
Response surface methodology
Solar photoelectro-Fenton
Sulfanilic acid

ABSTRACT

A central composite rotatable design and response surface methodology were used to optimize the experimental variables of the electro-Fenton (EF) and solar photoelectro-Fenton (SPEF) degradations of 2.5 L of sulfanilic acid solutions in 0.05 M $Na_2SO_4$. Electrolyses were performed with a pre-pilot flow plant containing a Pt/air diffusion reactor generating $H_2O_2$. In SPEF, it was coupled with a solar photoreactor under an UV irradiation intensity of ca. 31 W $m^{-2}$. Optimum variables of 100 mA $cm^{-2}$, 0.5 mM $Fe^{2+}$ and pH 4.0 were determined after 240 min of EF and 120 min of SPEF. Under these conditions, EF gave 47% of mineralization, whereas SPEF was much more powerful yielding 76% mineralization with 275 kWh $kg^{-1}$ total organic carbon (TOC) energy consumption and 52% current efficiency. Sulfanilic acid decayed at similar rate in both treatments following a pseudo-first-order kinetics. The final solution treated by EF contained a stable mixture of tartaric, acetic, oxalic and oxamic acids, which form Fe(III) complexes that are not attacked by hydroxyl radicals formed from $H_2O_2$ and added $Fe^{2+}$. The quick photolysis of these complexes by UV light of sunlight explains the higher oxidation power of SPEF. $NH_4^+$ was the main inorganic nitrogen ion released in both processes.



## 1. Introduction

Recently, electrochemical advanced oxidation processes (EAOPs) such as electro-Fenton (EF) and photoelectro-Fenton (PEF) have received great attention for water remediation because they can generate large amounts of oxidant hydroxyl radical (•OH) for an effective and fast mineralization of toxic organic pollutants to $CO_2$, water and inorganic ions [1,2]. In both EAOPs, $O_2$ or air gas is injected into either the reaction medium or directly at the cathode to generate $H_2O_2$ via reaction (1):

$$O_{2(g)} + 2H^+ + 2e^- \rightarrow H_2O_2 \quad (1)$$

$H_2O_2$ is efficiently produced at carbonaceous cathodes like carbon felt [3–9], activated carbon fiber [10], boron-doped diamond (BDD) [11] and carbon-polytetrafluoroethylene (PTFE) [2,12–18] and carbon nanotubes-PTFE [19–22] $O_2$ or air diffusion. The oxidizing power of $H_2O_2$ is enhanced by adding small amounts of $Fe^{2+}$ to form $Fe^{3+}$ and •OH in the bulk from Fenton's reaction (2):

$$Fe^{2+} + H_2O_2 + H^+ \rightarrow Fe^{3+} + {}^{\bullet}OH + H_2O \quad (2)$$

Reaction (2) is catalytic because it is primordially propagated from $Fe^{2+}$ regeneration by $Fe^{3+}$ reduction at the cathode [1]. When a one-compartment electrochemical reactor is used, organic pollutants can also be destroyed by adsorbed hydroxyl radical (M(•OH)) that is formed as intermediate of water discharge at the anode M by reaction (3) [23,24]:

$$M(H_2O) \rightarrow M({}^{\bullet}OH) + H^+ + e^- \quad (3)$$

In these systems, the BDD anode is preferred since it generates BDD(•OH) radicals with greater oxidation power than those of other electrodes like Pt and $PbO_2$ owing to its higher $O_2$-overpotential [24–27]. However, the Pt anode producing less potent Pt(•OH) radicals is widely employed because it yields more inexpensive treatments by the lower potential difference applied to the cell [25–27].

While the EF process destroys the organics with hydroxyl radicals mainly generated from reaction (2) giving dehydrogenated and/or hydroxylated derivatives that can in turn be mineralized,

* Corresponding author. Tel.: +34 934021223; fax: +34 934021231.
*E-mail address:* brillas@ub.edu (E. Brillas).

0304-3894/$ – see front matter © 2012 Elsevier B.V. All rights reserved.
http://dx.doi.org/10.1016/j.jhazmat.2012.04.053

it is found that the illumination of the solution with UVA light ($\lambda_{max}$ = 360 nm) in the PEF process accelerates the degradation of pollutants. This phenomenon is explained by: (i) the enhancement of $Fe^{2+}$ regeneration and •OH production by the photolytic reaction (4) and (ii) the photolysis of Fe(III) complexes with generated intermediates like carboxylic acids by reaction (5) [1–3,10,13,14,16–20]:

$$Fe(OH)^{2+} + h\nu \rightarrow Fe^{2+} + {}^{\bullet}OH \quad (4)$$

$$Fe(OOCR)^{2+} + h\nu \rightarrow Fe^{2+} + CO_2 + R^{\bullet} \quad (5)$$

Recently, our laboratory is developing the solar photoelectro-Fenton (SPEF) process that uses sunlight ($\lambda > 300$ nm) as an inexpensive and renewable energy source. The solar light is expected to improve the performance of artificial UVA lamps since it provides photons in the UV range of 300–400 nm, as well as in the visible ranges of 400–650 nm and 400–450 nm, which can also be absorbed for reactions (4) and (5), respectively [28,29]. In previous work, the SPEF degradation of the herbicide 4-chloro-2-methylphenoxyacetic acid [2], the pharmaceutical paracetamol [16] and several azo dyes [17,18] was tested, but more fundamental research is needed to clarify the mineralization power of this EAOP on other kinds of organics to check its possible application to industrial scale. In this way, we have undertaken a study on the SPEF process of sulfanilic acid (4-aminobenzenesulfonic acid), a toxic and carcinogenic compound widely used to synthesize pesticides, sulfonamide drugs, sulfonated azo dyes, species and food pigments. Sulfanilic acid has been detected in industrial dyes wastewaters, rivers and surface waters, where it can be formed from the anaerobic reduction of sulfonated azo dyes [30,31]. It can be very slowly biodegraded by different bacterial strains under aerobic conditions [32,33] and slowly destroyed by ozonation [34] and anodic oxidation [35]. Sulfanilic acid has been found as intermediate in the degradation of the antimicrobial sulfamethoxazole by $TiO_2$ photocatalysis [36] and Fenton reagent [37] and in the removal of the dye Acid Orange 7 by anodic oxidation [38] and EF [4].

This paper reports the SPEF degradation of 240 mg $L^{-1}$ sulfanilic acid solutions (equivalent to 100 mg $L^{-1}$ of total organic carbon (TOC)) using a 2.5 L pre-pilot flow plant containing a Pt/air diffusion cell coupled to a solar photoreactor. Comparative EF trials in the dark were made to assess the influence of solar irradiation. The optimum experimental variables for both processes were obtained with a central composite rotatable design (CCRD) coupled to response surface methodology (RSM) [39,40]. This statistical tool has been recently applied to describe treatments based on Fenton's reaction like chemical Fenton [40–42], photo-Fenton [42,43], solar photo-Fenton [44,45], EF [46,47] and SPEF [2,16]. However, no comparative studies between the EF and PEF degradations of organics have been previously reported. The sulfanilic acid decay and the evolution of generated carboxylic acids and released inorganic nitrogen ions for both optimized EAOPs were determined by chromatographic techniques to clarify the degradation processes.

## 2. Experimental

### 2.1. Chemicals

Sulfanilic acid (>99% purity) supplied by Sigma–Aldrich was used without further purification. Maleic, tartaric, acetic, oxamic and oxalic acids were of reagent grade from Panreac and Avocado. Heptahydrated ferrous sulfate used as catalyst and anhydrous sodium sulfate used as background electrolyte were analytical grade from Fluka. Sulfanilic acid solutions were prepared with deionised water and their pH was adjusted with analytical grade sulfuric acid supplied by Merck. Organic solvents and other chemicals employed were either HPLC or analytical grade from Merck, Fluka, Sigma–Aldrich and Avocado.

### 2.2. Apparatus and analytical procedures

The solution pH was measured with a Crison GLP 22 pH-meter. Aliquots of 5 mL withdrawn from electrolyzed solutions were neutralized at pH 7–8 to quench the degradation process and filtered with 0.45 μm PTFE filters from Whatman before analysis. The mineralization of sulfanilic acid solutions was monitored from their TOC decay, determined with a Shimadzu VCSN TOC analyzer. Total nitrogen (TN) was obtained with a Shimadzu TNM-1 unit coupled to the TOC analyzer.

The energy consumption per unit TOC mass (EC) was then calculated from Eq. (6) [16–18]:

$$EC(kWh\ kg^{-1}\ TOC) = \frac{1000 E_{cell} I t}{V_s \Delta(TOC)_{exp}} \quad (6)$$

where $E_{cell}$ is the average potential difference of the cell (V), $I$ is the current (A), $t$ is the electrolysis time (h), $V_s$ is the solution volume (L), $\Delta(TOC)_{exp}$ is the experimental TOC decay (mg $L^{-1}$) and 1000 is a conversion factor (mg $g^{-1}$).

The mineralization current efficiency (MCE) for each trial was estimated from Eq. (7) [48]:

$$MCE(\%) = \frac{n F V_s \Delta(TOC)_{exp}}{4.32 \times 10^7 m I t} \times 100 \quad (7)$$

where $F$ is the Faraday constant (96,487 C $mol^{-1}$), $4.32 \times 10^7$ is a conversion factor to homogenize units (3600 s $h^{-1}$ × 12,000 mg $mol^{-1}$) and $m$ is the number of carbon atoms of sulfanilic acid (6 atoms). The number of electrons ($n$) consumed per each molecule was taken as 28 assuming that sulfanilic acid is totally mineralized to carbon dioxide and sulfate and ammonium ions from reaction (8):

$$C_6H_7NO_3S + 13H_2O \rightarrow 6CO_2 + NH_4^+ + SO_4^{2-} + 29H^+ + 28e^- \quad (8)$$

The formation of sulfate ion is expected from the oxidation behavior of sulfonated compounds [1,4], whereas the initial nitrogen is mainly converted into $NH_4^+$ ion, as discussed below.

The decay kinetics for sulfanilic acid and the evolution of generated carboxylic acids were followed by ion-exclusion HPLC using a Waters 600 LC fitted with a Bio-Rad Aminex HPX 87H, 300 mm × 7.8 mm (i.d.), column at 35 °C, coupled with a Waters 996 photodiode array detector selected at $\lambda$ = 249 nm for sulfanilic acid and $\lambda$ = 210 nm for aliphatic carboxylic acids. This analysis was made by circulating a mobile phase of 4 mM $H_2SO_4$ at 0.6 mL $min^{-1}$ and well defined peaks with retention times of 6.9 min for oxalic acid, 8.2 min for maleic acid, 8.6 min for tartaric acid, 9.4 min for oxamic acid, 14.7 min for sulfanilic acid and 15.0 min for acetic acid were found. The $NH_4^+$ concentration was determined by ionic chromatography with a Shimadzu 10 Avp LC fitted with a Shodex IC YK-421, 125 mm × 4.6 mm (i.d.), cation column at 40 °C, coupled with a Shimadzu CDD 10 Avp conductivity detector. The mobile phase was a 5.0 mM tartaric acid, 2.0 mM dipicolinic acid, 24.2 mM boric acid and 1.5 mM crown ether solution at 1.0 mL $min^{-1}$. The $NO_3^-$ content was obtained using a Shim-Pack IC-A1S, 100 mm × 4.6 mm (i.d.), anion column at 40 °C, and a mobile phase of 2.4 mM tris(hydroxymethyl)aminomethane and 2.5 mM phthalic acid at 1.5 mL $min^{-1}$.

### 2.3. Pre-pilot flow plant

A sketch of the pre-pilot flow plant designed for the EF and SPEF processes is shown in Fig. 1. In each trial, 2.5 L of a sulfanilic acid solution were introduced in the reservoir and recirculated through the plant with a magnetic drive centrifugal pump from Iwaki at a liquid flow rate of 200 L $h^{-1}$ regulated by a flowmeter. The solution further passed through two heat exchangers to maintain the temperature at 35 °C, the electrochemical reactor

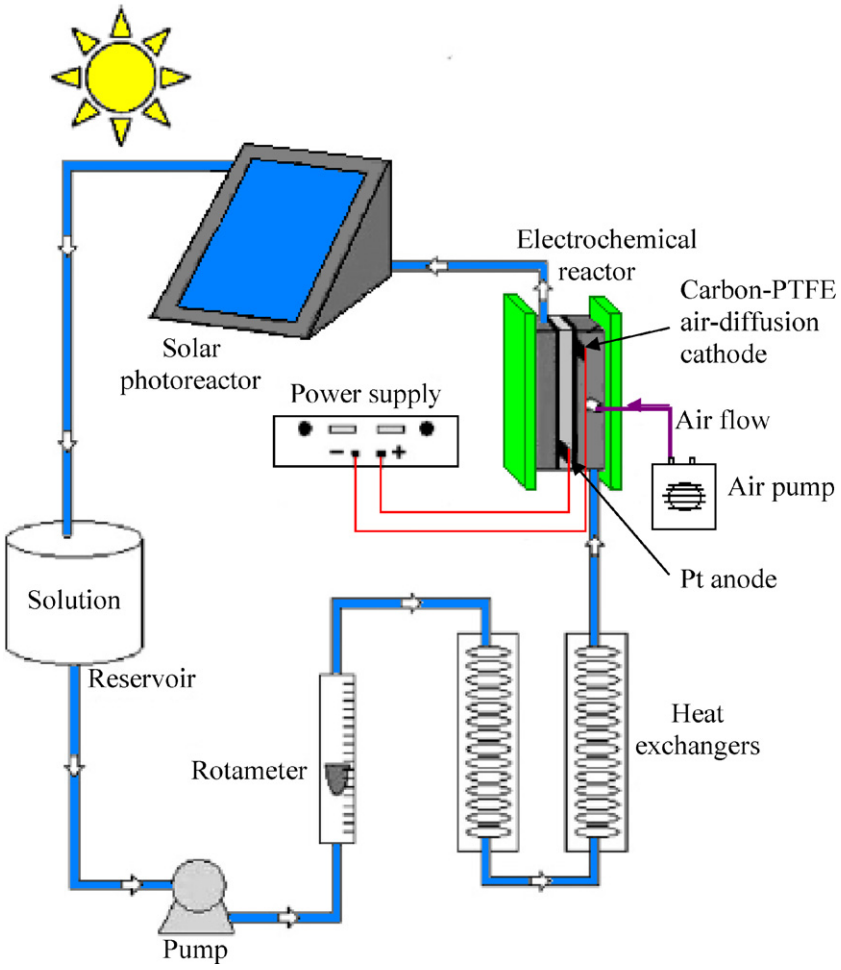


**Fig. 1.** Scheme of the experimental setup for the pre-pilot flow plant used for the electro-Fenton (EF) and solar photoelectro-Fenton (SPEF) degradations of 2.5 L of sulfanilic acid solutions. The electrochemical reactor was a filter-press Pt/air diffusion cell of 20 $cm^2$ electrode area. In SPEF, a solar photoreactor with 600 mL irradiation volume was used. In EF, the plant was covered with a black cloth.

and the solar photoreactor to finally return to the reservoir. The electrochemical reactor was a one-compartment filter-press cell with 20 $cm^2$ electrodes separated 1.2 cm. The anode was a Pt sheet (99.99% purity) from SEMPSA and the cathode was a carbon-PTFE air-diffusion electrode from E-TEK, which was fed with air pumped at an overpressure of 8.6 kPa to continuously produce $H_2O_2$ from reaction (1). The assays were carried out at constant current density provided by an Agilent 6552A DC power supply. The solar photoreactor was a polycarbonate box of 24 cm × 24 cm × 2.5 cm (600 mL of irradiated volume), with a mirror at the bottom and inclined 41° (equal to the latitude of our laboratory) to collect better the direct sun rays. SPEF trials were made for 210 min starting from the noon in sunny and clear days during summer of 2011 in Barcelona, Spain (latitude: 41°21′ N, longitude: 2°10′ E). The UV irradiation intensity (300–400 nm) supplied by sunlight was measured with a Kipp&Zonen CUV 5 radiometer. The EF experiments were performed for 300 min by covering the plant with a black cloth to avoid UV irradiation. Before degradation tests, the air diffusion cathode was activated by electrolyzing 2.5 L of 0.05 M $Na_2SO_4$ at pH 3.0 and 150 mA $cm^{-2}$ for 240 min.

### 2.4. Experimental design and response surface methodology

CCRD and RSM were applied to find the optimum conditions for the EF and SPEF degradations of sulfanilic acid. The responses analyzed were the variations of TOC, EC and MCE at 240 min of EF and 120 min of SPEF, and the three independent variables selected were current density ($j$), $Fe^{2+}$ concentration and pH. For each EAOP, the CCRD consisted of eight factorial points, six axial points and three central points, making 17 experiments [49]. The ranges of the variables were from 16 to 184 mA $cm^{-2}$ for current density, from 0.32 to 3.68 mM for $Fe^{2+}$ concentration and from 1.32 to 4.68 for pH. Five levels of each independent variable were taken as $x_i = -1.68$, $-1$, 0, 1 and 1.68, as can be seen in Table 1. The correlations between the responses and the independent variables were obtained by the following second-order model with a least-squares method [49]:

$$Y = \beta_0 + \sum_{i=1}^{k} \beta_i x_i + \sum_{i=1}^{k} \beta_{ii} x_i^2 + \sum_{i=1}^{k} \sum_{i\#j=1}^{k} \beta_{ij} x_i x_j + \varepsilon \quad (9)$$

where $Y$ is the response, $\beta_0$ is a constant coefficient, $\beta_i$, $\beta_{ii}$, and $\beta_{ij}$ are the coefficients for the linear, quadratic and interaction effects, respectively, $x_i$ and $x_j$ are the coded levels for the independent variables, $k$ is the number of independent variables and $\varepsilon$ is the random error.

Three replicates in the central point were made to estimate the pure error (runs 15–17 for EF and 32-34 for SPEF in Table 1). All the trials were randomly performed to minimize the effect of unexplained variability on the observed responses due to systematic errors [50]. The response surfaces [39,40,49] were generated

**Table 1**
Coded levels and real values for the central composite rotatable design and RSM analysis of the EF and SPEF treatments of 240 mg $L^{-1}$ sulfanilic acid solutions in 0.05 M $Na_2SO_4$ at 35 °C with a 2.5 L pre-pilot flow plant containing a Pt/air diffusion cell coupled to a solar photoreactor.

| Method | Run | Coded levels | | | Real values | | | Observed responses[d] | | | UV[e] ($W m^{-2}$) |
|---|---|---|---|---|---|---|---|---|---|---|---|
| | | $x_1$ | $x_2$ | $x_3$ | $X_1$[a] | $X_2$[b] | $X_3$[c] | TOC ($mg L^{-1}$) | EC ($kWh kg^{-1}$ TOC) | % MCE | |
| EF | 1 | −1 | −1 | −1 | 50 | 1.00 | 2.00 | 56.8 | 333.2 | 28.2 | – |
| | 2 | 1 | −1 | −1 | 150 | 1.00 | 2.00 | 49.6 | 1904.8 | 10.9 | – |
| | 3 | −1 | 1 | −1 | 50 | 3.00 | 2.00 | 70.1 | 480.8 | 19.5 | – |
| | 4 | 1 | 1 | −1 | 150 | 3.00 | 2.00 | 49.9 | 1916.6 | 10.9 | – |
| | 5 | −1 | −1 | 1 | 50 | 1.00 | 4.00 | 55.3 | 322.0 | 29.1 | – |
| | 6 | 1 | −1 | 1 | 150 | 1.00 | 4.00 | 44.5 | 1728.2 | 12.1 | – |
| | 7 | −1 | 1 | 1 | 50 | 3.00 | 4.00 | 66.5 | 429.9 | 21.8 | – |
| | 8 | 1 | 1 | 1 | 150 | 3.00 | 4.00 | 49.6 | 1905.5 | 10.9 | – |
| | 9 | −1.68 | 0 | 0 | 16 | 2.00 | 3.00 | 84.2 | 129.2 | 32.3 | – |
| | 10 | 1.68 | 0 | 0 | 184 | 2.00 | 3.00 | 47.4 | 2912.6 | 9.3 | – |
| | 11 | 0 | −1.68 | 0 | 100 | 0.32 | 3.00 | 56.2 | 1095.6 | 14.3 | – |
| | 12 | 0 | 1.68 | 0 | 100 | 3.68 | 3.00 | 53.6 | 1034.7 | 15.1 | – |
| | 13 | 0 | 0 | −1.68 | 100 | 2.00 | 1.32 | 56.9 | 1113.2 | 14.0 | – |
| | 14 | 0 | 0 | 1.68 | 100 | 2.00 | 4.68 | 51.4 | 987.3 | 15.8 | – |
| | 15 | 0 | 0 | 0 | 100 | 2.00 | 3.00 | 52.7 | 1013.7 | 15.4 | – |
| | 16 | 0 | 0 | 0 | 100 | 2.00 | 3.00 | 53.4 | 1028.9 | 15.2 | – |
| | 17 | 0 | 0 | 0 | 100 | 2.00 | 3.00 | 50.2 | 962.9 | 16.2 | – |
| SPEF | 18 | −1 | −1 | −1 | 50 | 1.00 | 2.00 | 79.6 | 293.8 | 26.6 | 31.1 |
| | 19 | 1 | −1 | −1 | 150 | 1.00 | 2.00 | 29.9 | 634.1 | 30.4 | 32.2 |
| | 20 | −1 | 1 | −1 | 50 | 3.00 | 2.00 | 86.6 | 446.8 | 17.5 | 32.5 |
| | 21 | 1 | 1 | −1 | 150 | 3.00 | 2.00 | 14.2 | 517.7 | 37.3 | 30.5 |
| | 22 | −1 | −1 | 1 | 50 | 1.00 | 4.00 | 57.0 | 109.8 | 55.9 | 31.8 |
| | 23 | 1 | −1 | 1 | 150 | 1.00 | 4.00 | 15.9 | 528.5 | 36.5 | 31.4 |
| | 24 | −1 | 1 | 1 | 50 | 3.00 | 4.00 | 82.8 | 338.6 | 22.4 | 30.6 |
| | 25 | 1 | 1 | 1 | 150 | 3.00 | 4.00 | 21.0 | 562.2 | 34.3 | 30.2 |
| | 26 | −1.68 | 0 | 0 | 16 | 2.00 | 3.00 | 90.3 | 105.4 | 39.6 | 31.3 |
| | 27 | 1.68 | 0 | 0 | 184 | 2.00 | 3.00 | 19.8 | 752.6 | 28.4 | 32.1 |
| | 28 | 0 | −1.68 | 0 | 100 | 0.32 | 3.00 | 34.9 | 307.2 | 42.4 | 30.7 |
| | 29 | 0 | 1.68 | 0 | 100 | 3.68 | 3.00 | 43.7 | 354.9 | 36.7 | 30.4 |
| | 30 | 0 | 0 | −1.68 | 100 | 2.00 | 1.32 | 63.8 | 542.9 | 23.6 | 31.2 |
| | 31 | 0 | 0 | 1.68 | 100 | 2.00 | 4.68 | 29.6 | 283.9 | 45.9 | 30.2 |
| | 32 | 0 | 0 | 0 | 100 | 2.00 | 3.00 | 41.6 | 343.6 | 38.0 | 32.4 |
| | 33 | 0 | 0 | 0 | 100 | 2.00 | 3.00 | 39.2 | 329.0 | 39.6 | 30.7 |
| | 34 | 0 | 0 | 0 | 100 | 2.00 | 3.00 | 37.0 | 316.1 | 41.0 | 31.0 |

[a] Current density ($mA cm^{-2}$).
[b] $Fe^{2+}$ concentration (mM).
[c] pH.
[d] Obtained at 240 min of EF or 120 min of SPEF.
[e] Average UV irradiation intensity supplied by sunlight for 120 min of SPEF.

by a StatSoft STATISTICA v6 program to determine the best conditions for sulfanilic acid mineralization. The polynomial models developed were statistically validated by means of analysis of variance (ANOVA), checking their statistical significances from the *F*-test and their fit quality from the coefficients of determination $R^2$.

## 3. Results and discussion

### 3.1. EF and SPEF degradations of sulfanilic acid solutions

Sulfanilic acid solutions were comparatively degraded by EF and SPEF in the pre-pilot flow plant. The initial colorless solutions acquired rapidly a dark brown color, which further changed to orange and yellow, becoming colorless again in 60–80 min of both treatments. This suggests the formation of colored conjugated intermediates that are progressively removed by •OH [1,2]. The solution pH generally decreased during electrolysis by the formation of acidic derivatives like carboxylic acids and then, small volumes of NaOH 1.0 M were added to the solution to regulate its pH to its initial value. The degradation rate in EF was found much lower than that of SPEF under comparable conditions, as expected from the efficient synergistic action of sunlight. Electrolysis times of 240 min for EF and 120 min for SPEF were then taken to optimize the independent variables from CCRD. Table 1 summarizes the observed responses under these conditions for all coded levels tested. A quite similar average UV irradiation intensity between 30.2 and 32.4 $W m^{-2}$ was supplied to the solar photoreactor during all SPEF treatments.

### 3.2. Influence of independent experimental variables on the EF and SPEF processes

The analysis of the observed responses (TOC, MCE and EC) given in Table 1 using Eq. (9) yielded the following adjusted second-order models at 95% confidence level for EF at 240 min:

$$TOC_{EF\text{-}240} = 52.27 - 8.55x_1 + 1.86x_2 - 1.45x_3 + 4.11x_1^2 - 2.38x_1x_2 + 0.35x_2x_3 \quad (10)$$

$$EC_{EF\text{-}240} = 1008 + 774x_1 + 25.05x_2 - 33.79x_3 + 161.9x_1^2 - 15.69x_1x_3 + 15.72x_2x_3 \quad (11)$$

$$MCE_{EF\text{-}240} = 15.55 - 6.77x_1 - 1.15x_2 + 0.55x_3 + 2.06x_1^2 + 1.85x_1x_2 \quad (12)$$

and for SPEF at 120 min:

$$TOC_{SPEF\text{-}120} = 39.24 - 25.13x_1 + 2.69x_2 - 6.67x_3 + 5.77x_1^2 + 2.82x_3^2 - 5.43x_1x_2 + 2.39x_1x_3 + 4.95x_2x_3 \quad (13)$$

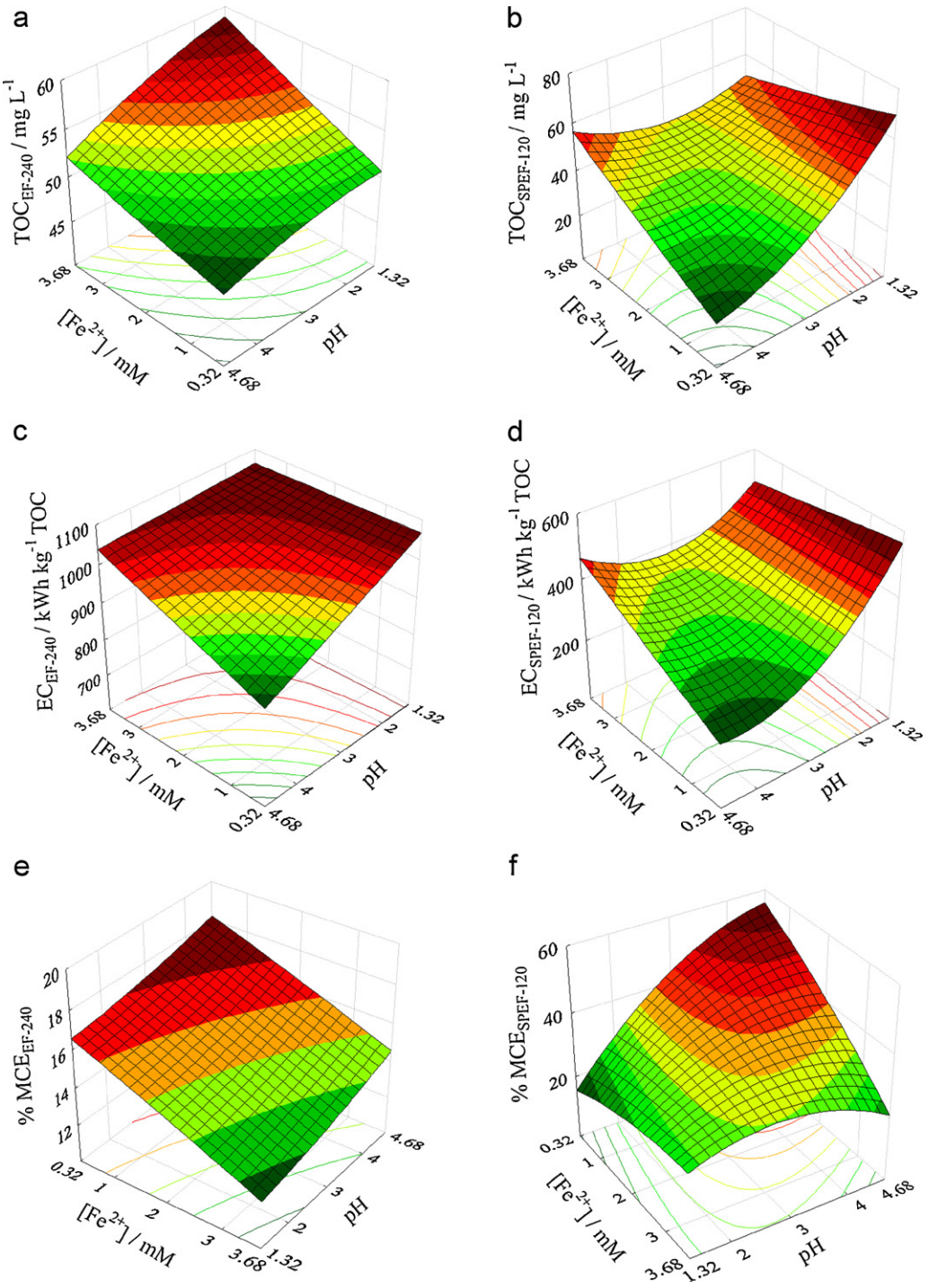


**Fig. 2.** Comparative response surfaces generated from the CCRD method after the EF and SPEF treatments of 2.5 L of 240 mg $L^{-1}$ sulfanilic acid solutions in 0.05 M $Na_2SO_4$ using a pre-pilot flow plant at 35 °C and liquid flow rate of 200 L $h^{-1}$. (a) Total organic carbon (TOC) after 240 min of EF, (b) TOC after 120 min of SPEF, (c) energy consumption per unit TOC mass (EC) after 240 min of EF, (d) EC after 120 min of SPEF, (e) mineralization current efficiency (MCE) after 240 min of EF and (f) MCE after 120 min of SPEF. All surfaces are presented for $Fe^{2+}$ concentration vs pH.

$$EC_{SPEF-120} = 327.2 + 147.7x_1 + 27.78x_2 - 57.75x_3 + 39.75x_1^2 + 38.04x_3^2 - 58.04x_1x_2 + 28.88x_1x_3 + 28.86x_2x_3 \quad (14)$$

$$MCE_{SPEF-120} = 39.75 - 3.48x_2 + 5.49x_3 - 2.69x_1^2 - 2.43x_3^2 + 5.91x_1x_2 - 3.90x_1x_3 - 4.18x_2x_3 \quad (15)$$

where $x_1$, $x_2$ and $x_3$ are the current density, $Fe^{2+}$ concentration and pH, respectively. In Eqs. (10)–(15) only the significant terms determined from ANOVA are included.

The high negative contribution of $x_1$ in Eqs. (10) and (13) evidences a faster TOC abatement with increasing $j$ for both EAOPs. This behavior is accounted for by the generation of more amounts of •OH from Fenton's reaction (2) owing to the greater $H_2O_2$ generation by reaction (1) [14,17,18]. The rise in current density caused a large effect on energy consumption, as reflected by the high

positive coefficients for $x_1$ and $x_1^2$ in Eqs. (11) and (14). In fact, $EC_{EF\text{-}240}$ increased strongly from 16 to 184 mA cm$^{-2}$, whereas a much less pronounced rise from 16 to 100 mA cm$^{-2}$ occurred for $EC_{SPEF\text{-}120}$ probably due to the more efficient loss of $TOC_{SPEF\text{-}120}$ under the action of sunlight at lower current densities. The influence of $j$ was also significant for $MCE_{EF\text{-}240}$ due to the negative value of $x_1$ in Eq. (12) and for $MCE_{SPEF\text{-}240}$ because of the greater negative contribution of $x_1^2$ in Eq. (15). Both efficiencies decreased with increasing current density, which can be related to the loss of reactive •OH by the enhancement of its non-oxidizing reactions involving, for example, its attack on $H_2O_2$ by reaction (16) giving the weaker oxidant hydroperoxyl radical ($HO_2$•) [1], thus producing a decrease in organic events.

$$H_2O_2 + {}^{\bullet}OH \rightarrow HO_2{}^{\bullet} + H_2O \quad (16)$$

Eqs. (10)–(15) also point to the existence of a notable influence of $Fe^{2+}$ concentration and pH on the TOC and MCE values of both EAOPs, which is much less significant for the corresponding EC. This can be observed in the response surfaces presented in Fig. 2. They confirm that SPEF is more powerful and more economic than EF since $TOC_{SPEF\text{-}120} > TOC_{EF\text{-}240}$, $EC_{SPEF\text{-}120} < EC_{EF\text{-}240}$ and $MCE_{SPEF\text{-}120} > MCE_{EF\text{-}240}$ under comparable conditions. Fig. 2a and b shows that the maximum sulfanilic acid mineralization was always achieved for $Fe^{2+}$ contents up to 0.5 mM, while the use of higher concentrations yielded decreasing $TOC_{EF\text{-}240}$ and $TOC_{SPEF\text{-}120}$ abatements. Under these conditions, the excess of added $Fe^{2+}$ is expected to rapidly react with •OH by reaction (17) [1,2], decreasing the quantity of this radical to oxidize organics and hence, inhibiting the mineralization process.

$$Fe^{2+} + {}^{\bullet}OH \rightarrow Fe^{3+} + OH^- \quad (17)$$

Fig. 2a and b also illustrates that the best pH for both TOC removals was reached between 3.0 and 4.0, close to the optimum pH 2.8 for Fenton's reaction (2) [1]. Besides, Fig. 2c–f shows that the lower $EC_{EF\text{-}240}$ and $EC_{SPEF\text{-}120}$, as well as the higher $MCE_{EF\text{-}240}$ and $MCE_{SPEF\text{-}120}$ values, were found again for $Fe^{2+}$ contents up to 0.5 mM and pH ca. 4.0. This behavior corroborates the consumption of •OH by higher concentrations of $Fe^{2+}$ via reaction (17). The lower effectiveness of both processes at pH < 2.5 can be related to the formation of the peroxonium ion ($H_3O_2^+$) by reaction (18) [51–53]:

$$H_2O_2 + H^+ \rightarrow H_3O_2^+ \quad (18)$$

The progressive generation of more $H_3O_2^+$ with lowering pH makes the electrogenerated $H_2O_2$ more electrophilic, thereby enhancing its stability and reducing its reactivity with $Fe^{2+}$ in Fenton's reaction (2). At pH > 4.0, the precipitation of $Fe^{3+}$ and its hard reduction to $Fe^{2+}$ produces less •OH from Fenton's reaction (2), explaining the lower TOC removal and MCE obtained.

### 3.3. Validation of the quadratic models

The Fisher distribution ($F$-test) from ANOVA was used to statistically validate the significance of regressions and the lack of fit for the quadratic models of Eqs. (10)–(15). The significance of the six models was then evaluated from the ratio between the mean squares of the regression and residuals (difference between observed and predicted values), whereas their adjustment was assessed from the ratio between the mean squares of lack of fit and pure error. The $F$-ratio calculated for the regressions was 6.06 for $TOC_{EF\text{-}240}$, 79.68 for $EC_{EF\text{-}240}$, 23.85 for $MCE_{EF\text{-}240}$, 26.36 for $TOC_{SPEF\text{-}120}$, 20.54 for $EC_{SPEF\text{-}120}$ and 4.68 for $MCE_{SPEF\text{-}120}$. All these values were greater than 3.29 theoretically calculated for 95% confidence level, corroborating that the developed models are statistically significant [50]. The $F$-ratio calculated for the lack of fit of the above models was 11.69 for $TOC_{EF\text{-}240}$, 13.56 for $EC_{EF\text{-}240}$, 15.40 for $MCE_{EF\text{-}240}$, 11.02 for $TOC_{SPEF\text{-}120}$, 16.29 for $EC_{SPEF\text{-}120}$ and 17.88 for $MCE_{SPEF\text{-}120}$, lower than 19.30 tabulated for 95% confidence level, indicating that they are satisfactory without evidencing a lack of fit [49,50]. As an example, Figs. 3a and 4a show that the residuals for $EC_{EF\text{-}240}$ and $EC_{SPEF\text{-}120}$ are randomly distributed around the mean in front of predicted values due to the good agreement of the models, thereby discarding systematic errors. Similar residual-predicted plots were obtained for the TOC and MCE values of both EAOPs. Moreover, good linear correlations between the predicted and observed values for $EC_{EF\text{-}240}$ (Fig. 3b) and $EC_{SPEF\text{-}120}$ (Fig. 4b), with respective $R^2$ values of 0.990 and 0.964, were found. The same behavior was determined for the predicted-observed plots for $TOC_{EF\text{-}240}$, $MCE_{EF\text{-}240}$, $TOC_{SPEF\text{-}120}$ and $MCE_{SPEF\text{-}120}$, with $R^2$ values of 0.898, 0.968, 0.971 and 0.858, respectively. The fact that the determination coefficients are close to unity also confirms the statistical significance of the six quadratic models developed.

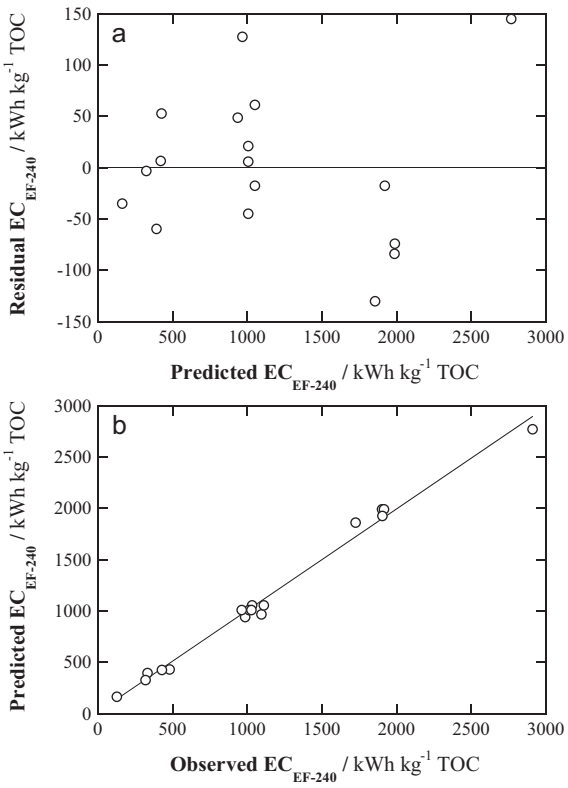


**Fig. 3.** (a) Residual-predicted and (b) predicted-observed plots determined for the energy consumption per unit TOC mass at 240 min of the EF degradation of 2.5 L of 240 mg L$^{-1}$ of sulfanilic acid in 0.05 M $Na_2SO_4$ in the pre-pilot flow plant in the dark at 35 °C and liquid flow rate of 200 L h$^{-1}$. Predicted values were obtained from Eq. (11) and residual values as the difference between the observed and predicted ones.

### 3.4. Optimization of the EF and SPEF treatments of sulfanilic acid

The optimum conditions for the EF and SPEF degradations of 240 mg L$^{-1}$ sulfanilic acid solutions were established from the above RSM results considering that high TOC removal with low EC and good mineralization current efficiency have to be achieved. Our results indicate that the optimum mineralization takes place with similar independent variables in EF at 240 min and SPEF at 120 min. So, acceptable $TOC_{EF\text{-}240}$ and $TOC_{SPEF\text{-}120}$ values were obtained at 100 mA cm$^{-2}$, while pH ca. 4.0 and $Fe^{2+}$ concentrations near 0.5 mM yielded minimum $EC_{EF\text{-}240}$ and $EC_{SPEF\text{-}120}$ with maximum $MCE_{EF\text{-}240}$ and $MCE_{SPEF\text{-}120}$. On this basis, 100 mA cm$^{-2}$ ($x_1 = 0$), 0.5 mM $Fe^{2+}$ ($x_2 = -1.5$) and pH 4.0 ($x_3 = 1$) were set as the best experimental conditions for both EAOPs.

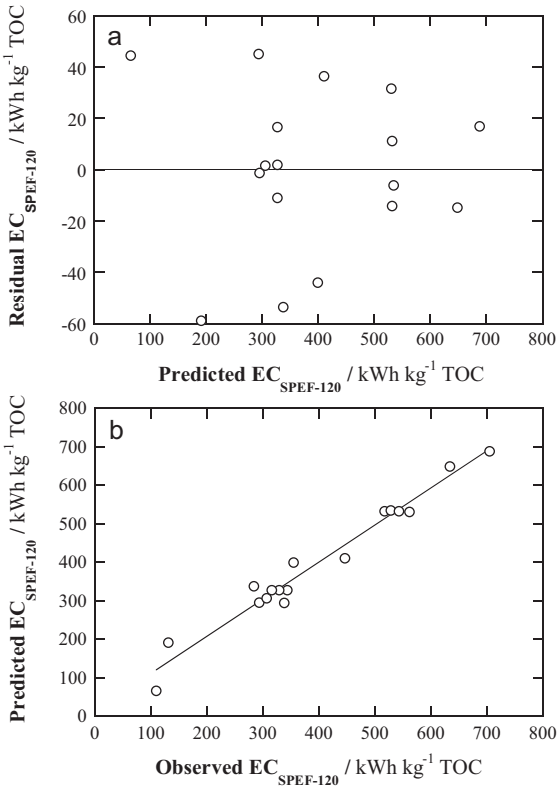


**Fig. 4.** (a) Residual-predicted and (b) predicted-observed plots obtained for the energy consumption per unit TOC mass at 120 min of the SPEF treatment of 2.5 L of 240 mg $L^{-1}$ of a sulfanilic acid solution in 0.05 M $Na_2SO_4$ in the solar pre-pilot flow plant at 35 °C and liquid flow rate of 200 L $h^{-1}$. Predicted values from Eq. (14).

Fig. 5a, b and c depicts the time course for TOC, EC and MCE, respectively, obtained during the above optimum EF and SPEF processes. TOC was always removed gradually, although much more rapidly for SPEF reaching 9 mg $L^{-1}$ at 210 min than for EF attaining 50 mg $L^{-1}$ at 300 min. Lower energy consumptions and greater efficiencies were then obtained for SPEF. Fig. 5b shows a continuous increase in EC for EF, whereas it attained a minimal just at 120 min of SPEF. The opposite trends can be observed in Fig. 5c for MCE. Fig. 5a–c evidences a similar change of TOC, EC and MCE for 60 min of EF and SPEF, suggesting an initial slow production of intermediates that are photolyzed by solar irradiation in SPEF. At 240 min of EF, TOC was reduced to 53 mg $L^{-1}$ with EC of 936 kWh $kg^{-1}$ TOC and MCE of 15%, in good agreement with 48 mg $L^{-1}$, 910 kWh $kg^{-1}$ TOC and 17% predicted from Eqs. (10), (11) and (12), respectively. At 120 min of SPEF, experimental values of 24 mg $L^{-1}$ for TOC, 275 kWh $kg^{-1}$ TOC for EC and 52% for MCE, close to 24 mg $L^{-1}$, 243 kWh $kg^{-1}$ TOC and 52% obtained from Eq. (13), (14) and (15), respectively, were determined. These findings evidence the excellent description of both processes by the quadratic models developed by RSM.

### 3.5. Decay kinetics for sulfanilic acid and evolution of its oxidation products

The kinetics of the reaction between sulfanilic acid and generated •OH in EF and SPEF was followed by reversed-phase HPLC. Previous blank experiments discarded the direct photolysis of this compound by sunlight because its content did not vary after 60 min of recirculation of the 240 mg $L^{-1}$ solution through the pre-pilot flow plant without passing current.

Fig. 6 shows a quick decay of the 240 mg $L^{-1}$ of sulfanilic acid, at similar rate for EF and SPEF, under optimized conditions,

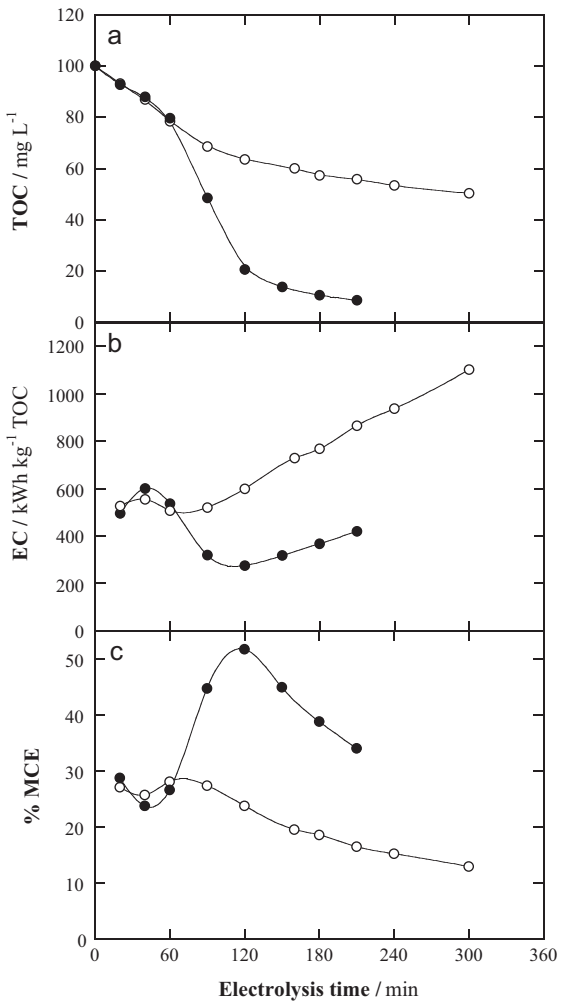


**Fig. 5.** (a) TOC abatement and variations of (b) EC and (c) MCE with electrolysis time for the (○) EF and (●) SPEF treatments of 2.5 L of a 240 mg $L^{-1}$ sulfanilic acid solution in 0.05 M $Na_2SO_4$ in the pre-pilot flow plant at 35 °C and liquid flow rate of 200 L $h^{-1}$ under the optimum conditions of 100 mA $cm^{-2}$, 0.50 mM $Fe^{2+}$ and pH 4.0 found by RSM.

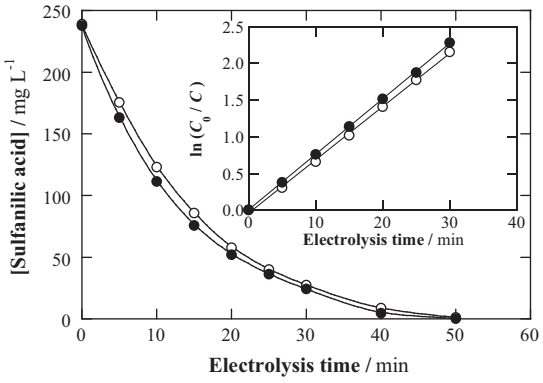


**Fig. 6.** Sulfanilic acid concentration decay during the optimized (○) EF and (●) SPEF treatments of 2.5 L of 240 mg $L^{-1}$ sulfanilic acid in 0.05 M $Na_2SO_4$ in the pre-pilot flow plant at 100 mA $cm^{-2}$, 0.50 mM $Fe^{2+}$, pH 4.0, 35 °C and liquid flow rate of 200 L $h^{-1}$. The inset panel depicts the corresponding kinetic analysis considering a pseudo-first-order reaction for sulfanilic acid.

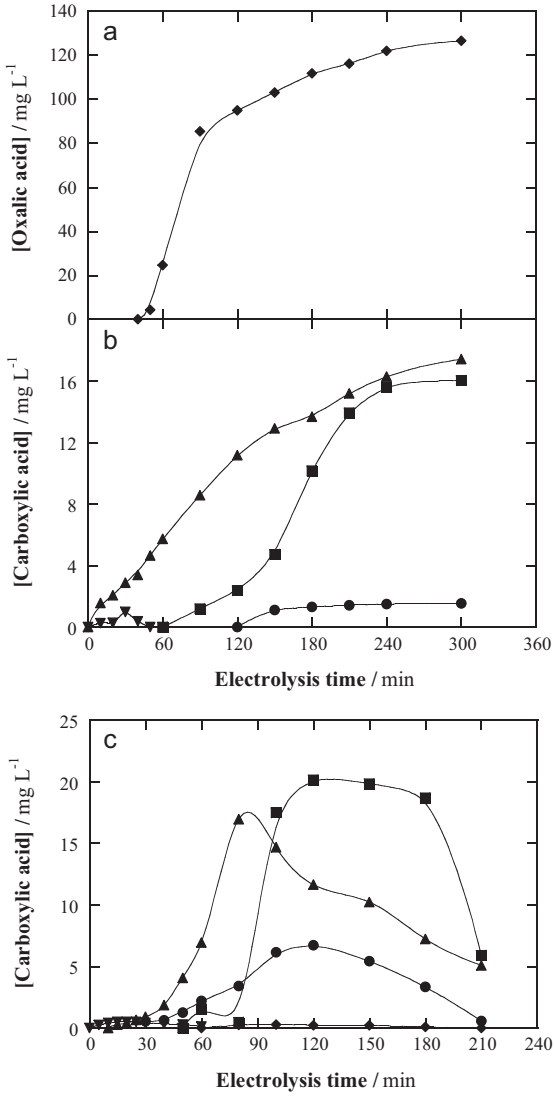


**Fig. 7.** Evolution of the concentration of: (▼) maleic, (●) tartaric, (■) acetic, (▲) oxamic and (♦) oxalic acids detected during the (a and b) EF and (c) SPEF degradations of 2.5 L of a 240 mg L$^{-1}$ sulfanilic acid solution in 0.05 M $Na_2SO_4$ in the pre-pilot flow plant at 35 °C and liquid flow rate of 200 L h$^{-1}$ under the optimum conditions of 100 mA cm$^{-2}$, 0.50 mM $Fe^{2+}$ and pH 4.0.

disappearing in 50 min. This evidences that the compound mainly reacts with •OH formed from Fenton's reaction (2) with little participation of photolytic reaction (4). The inset panel of Fig. 6 illustrates the excellent fitting of the above concentration decays with a pseudo-first-order kinetic equation. From this analysis, apparent rate constants of $1.21 \times 10^{-3}$ s$^{-1}$ ($R^2 = 0.998$) for EF and $1.26 \times 10^{-3}$ s$^{-1}$ ($R^2 = 0.999$) for SPEF were found. This behavior is indicative of the production of a constant amount of •OH during both treatments, at least while sulfanilic acid is removed.

Ion-exclusion HPLC of the electrolyzed solutions exhibited peaks related to maleic, tartaric, acetic, oxalic and oxamic acids. The three former acids can be formed from the cleavage of the benzenic ring of aromatic intermediates, then being oxidized to oxalic acid [13,14,16]. Oxamic acid is expected to proceed from the decomposition of intermediates containing the —$NH_2$ group. Oxalic and oxamic acids are ultimate acids that are directly mineralized to $CO_2$ [1]. Note that $Fe^{3+}$ generated from Fenton's reaction (2) forms complexes with all these acids under the optimized EF and SPEF conditions [2,16].

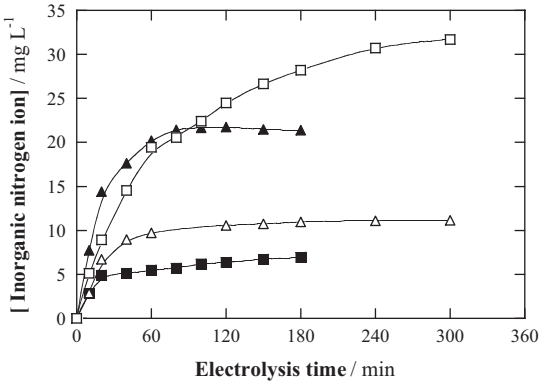


**Fig. 8.** Time course of (△, ▲) $NH_4^+$ and (□, ■) $NO_3^-$ ions detected during the optimized mineralization process of 2.5 L of a 240 mg L$^{-1}$ sulfanilic acid solution in 0.05 M $Na_2SO_4$ in the pre-pilot flow plant at 35 °C and liquid flow rate of 200 L h$^{-1}$ by (△, □) EF and (▲, ■) SPEF at 100 mA cm$^{-2}$, 0.50 mM $Fe^{2+}$ and pH 4.0.

Fig. 7a and b illustrates the large accumulation of all detected acids during EF, except maleic acid that is removed in 50 min after reaching a maximum of 1 mg L$^{-1}$. This means that Fe(III)–maleate complexes are oxidized by •OH, but the Fe(III) complexes of the other acids are not attacked by this radical. So, 126 mg L$^{-1}$ of oxalic acid and much smaller contents of 17, 16 and 1.5 mg L$^{-1}$ of oxamic, acetic and tartaric acids, respectively, were accumulated after 300 min of electrolysis. A simple mass balance reveals that the detected acids in the final solution correspond to 45 mg L$^{-1}$ TOC, a value slightly lower than 50 mg L$^{-1}$ found experimentally (Fig. 5a), This indicates that the major proportion (ca. 90%) of remaining by-products in EF are recalcitrant aliphatic carboxylic acids. A very different behavior can be observed in Fig. 7c for SPEF, since oxalic acid was not practically accumulated and the concentrations of oxamic, acetic and tartaric acids were drastically reduced at 210 min. These remaining acids represented about 4 mg L$^{-1}$ TOC, i.e., ca. 50% of 9 mg L$^{-1}$ TOC present in the final solution treated by SPEF (Fig. 5a). These findings demonstrate the high effectiveness of UV light supplied by solar irradiation to rapidly remove the Fe(III)–carboxylate complexes by reaction (5), strongly enhancing the oxidation power of SPEF in relation to EF.

TN analysis of electrolyzed solutions revealed that the 19.4 mg L$^{-1}$ of initial N contained in 240 mg L$^{-1}$ of sulfanilic acid were also present at the end of the optimized EF and SPEF treatments. Ionic chromatography confirmed the release of N as $NH_4^+$ ion in larger proportion than as $NO_3^-$ ion in both processes, as given in reaction (8). Fig. 8 shows the accumulation of 11.1 mg L$^{-1}$ $NH_4^+$ (45% of initial N) and 31.7 mg L$^{-1}$ $NO_3^-$ (37% of initial N) after 300 min of EF and 21.4 mg L$^{-1}$ $NH_4^+$ (86% of initial N) and 6.9 mg L$^{-1}$ $NO_3^-$ (8% of initial N) after 210 min of SPEF. The remaining N in solution was mainly oxamic acid, corresponding to 13% and 4% of initial N for EF and SPEF, respectively (Fig. 7b and c). These findings suggest that solar irradiation favors the release of $NH_4^+$ ion from photolysis of a large proportion of *N*-intermediates in SPEF, while the slower destruction of these compounds with •OH in the dark yields much more amount of $NO_3^-$ ion in EF. A high increase in $NH_4^+$ ion content with respect to that of $NO_3^-$ ion has also been reported for the SPEF treatment of the dye Acid Yellow 36 compared with the similar EF process [17].

## 4. Conclusions

The application of a central composite rotatable design coupled with response surface methodology gave the same optimized variables for the EF and SPEF degradations of 240 mg L$^{-1}$ of sulfanilic acid in 0.05 M $Na_2SO_4$ at 35 °C. Trials were performed with a 2.5 L

pre-pilot flow plant containing a Pt/air diffusion reactor, coupled with a solar photoreactor in SPEF submitted to an average UV irradiation intensity of about 31 W $m^{-2}$. The optimum variables were 100 mA $cm^{-2}$, 0.5 mM $Fe^{2+}$ and pH 4.0 determined after 240 min of EF and 120 min of SPEF. Under these conditions, TOC was reduced by 47% in EF and in much larger extent of 76% in SPEF, where it attained a minimum energy consumption of 275 kWh $kg^{-1}$ TOC with a maximum mineralization current efficiency of 52%. The SPEF process was then much more powerful and more economic by the synergistic action of sunlight. Sulfanilic acid decayed at similar rate in both EAOPs following a pseudo-first-order kinetics. Tartaric, acetic, oxalic and oxamic acids were the main components of the final solution treated by EF since their Fe(III) complexes are not destroyed by •OH. In SPEF, these complexes were largely photolyzed by the UV light of solar irradiation, thus explaining its higher oxidation power. The initial N was mainly released as $NH_4^+$ ion in both processes, although $NO_3^-$ ion was produced more largely in EF.

## Acknowledgements

The authors thank the financial support from MICINN (Ministerio de Ciencia e Innovación, Spain) through project CTQ 2010-16164/BQU, co-financed with Feder funds. The grants awarded to A. El-Ghenymy and S. Garcia-Segura by MEC (Ministerio de Educación y Ciencia, Spain) are also acknowledged.

## References

[1] E. Brillas, I. Sirés, M.A. Oturan, Electro-Fenton process and related electrochemical technologies based on Fenton's reaction chemistry, Chem. Rev. 109 (2009) 6570–6631.
[2] S. Garcia-Segura, L.C. Almeida, N. Bocchi, E. Brillas, Solar photoelectro-Fenton degradation of the herbicide 4-chloro-2-methylphenoxyacetic acid optimized by response surface methodology, J. Hazard. Mater. 194 (2011) 109–118.
[3] S. Irmak, H. Yavuz, I. Halil, O. Erbatur, Degradation of 4-chloro-2-methylphenol in aqueous solution by electro-Fenton and photoelectro-Fenton processes, Appl. Catal. B: Environ. 63 (2006) 243–248.
[4] S. Hammami, N. Oturan, N. Bellakhal, M. Dachraoui, M.A. Oturan, Oxidative degradation of direct Orange 61 by electro-Fenton process using a carbon felt electrode: application of the experimental design methodology, J. Electroanal. Chem. 610 (2007) 75–84.
[5] A. Özcan, Y. Şahin, K. Savaş, M.A. Oturan, Degradation of picloram by the electro-Fenton process, J. Hazard. Mater. 153 (2008) 718–727.
[6] A. Dhaouadi, N. Adhoum, Degradation of paraquat herbicide by electrochemical advanced oxidation methods, J. Electroanal. Chem. 637 (2009) 33–42.
[7] N. Oturan, M. Panizza, M.A. Oturan, Cold incineration of chlorophenols in aqueous solution by advanced electrochemical process electro-Fenton. Effect of number and position of chlorine atoms on the degradation kinetics, J. Phys. Chem. A 113 (2009) 10988–10993.
[8] M.A. Oturan, M.C. Edelahi, N. Oturan, K. El Kacemi, J.J. Aaron, Kinetics of oxidative degradation/mineralization pathways of the phenylurea herbicides diuron, monuron and fenuron in water during application of the electro-Fenton process, Appl. Catal. B: Environ. 97 (2010) 82–89.
[9] M. Panizza, M.A. Oturan, Degradation of Alizarin Red by electro-Fenton process using a graphite-felt cathode, Electrochim. Acta 56 (2011) 7084–7087.
[10] A. Wang, J. Qu, H. Liu, J. Ru, Mineralization of an azo dye Acid Red 14 by photoelectro-Fenton process using an activated carbon fiber cathode, Appl. Catal. B: Environ. 84 (2008) 393–399.
[11] K. Cruz-Gonzalez, O. Torres-Lopez, A. Garcia-Leon, J.L. Guzman-Mar, L.H. Reyes, A. Hernandez-Ramirez, J.M. Peralta-Hernandez, Determination of optimum operating parameters for Acid Yellow 36 decolorization by electro-Fenton process using BDD cathode, Chem. Eng. J. 160 (2010) 199–206.
[12] B. Boye, M.M. Dieng, E. Brillas, Electrochemical degradation of 2,4,5-trichlorophenoxyacetic acid in aqueous medium by peroxi-coagulation. Effect of pH and UV light, Electrochim. Acta 48 (2003) 781–790.
[13] C. Flox, P.L. Cabot, F. Centellas, J.A. Garrido, R.M. Rodríguez, C. Arias, E. Brillas, Solar photoelectro-Fenton degradation of cresols using a flow reactor with a boron-doped diamond anode, Appl. Catal. B: Environ. 75 (2007) 17–28.
[14] M. Skoumal, R.M. Rodríguez, P.L. Cabot, F. Centellas, J.A. Garrido, C. Arias, E. Brillas, Electro-Fenton, UVA photoelectro-Fenton and solar photoelectro-Fenton degradation of the drug ibuprofen in acid aqueous medium using platinum and boron-doped diamond anodes, Electrochim. Acta 54 (2009) 2077–2085.
[15] M. Panizza, G. Cerisola, Electro-Fenton degradation of synthetic dyes, Water Res. 43 (2009) 339–344.
[16] L.C. Almeida, S. Garcia-Segura, N. Bocchi, E. Brillas, Solar photoelectro-Fenton degradation of paracetamol using a flow plant with a Pt/air-diffusion cell coupled with a compound parabolic collector: process optimization by response surface methodology, Appl. Catal. B: Environ. 103 (2011) 21–30.
[17] E.J. Ruiz, C. Arias, E. Brillas, A. Hernández-Ramírez, J.M. Peralta-Hernández, Mineralization of Acid Yellow 36 azo dye by electro-Fenton and solar photoelectro-Fenton processes with a boron-doped diamond anode, Chemosphere 82 (2011) 495–501.
[18] R. Salazar, S. Garcia-Segura, M.S. Ureta-Zañartu, E. Brillas, Degradation of disperse azo dyes from waters by solar photoelectro-Fenton, Electrochim. Acta 56 (2011) 6371–6379.
[19] M. Zarei, A.R. Khataee, R. Ordikhani-Seyedlar, M. Fathinia, Photoelectro-Fenton combined with photocatalytic process for degradation of an azo dye using supported $TiO_2$ nanoparticles and carbon nanotube cathode: neural network modeling, Electrochim. Acta 55 (2010) 7259–7265.
[20] A.R. Khataee, M. Zarei, L. Moradkhannejhad, Application of response surface methodology for optimization of azo dye removal by oxalate catalyzed photoelectro-Fenton process using carbon nanotube-PTFE cathode, Desalination 258 (2010) 112–119.
[21] M. Zarei, A. Niaei, D. Salari, A.R. Khataee, Application of response surface methodology for optimization of peroxi-coagulation of textile dye solution using carbon nanotube-PTFE cathode, J. Hazard. Mater. 173 (2010) 544–551.
[22] A.R. Khataee, M. Safarpour, M. Zarei, S. Aber, Electrochemical generation of $H_2O_2$ using immobilized carbon nanotubes on graphite electrode fed with air: investigation of operational parameters, J. Electroanal. Chem. 169 (2011) 63–68.
[23] C.A. Martínez-Huitle, E. Brillas, Electrochemical alternatives for drinking water disinfection, Angew. Chem. Int. Ed. 47 (2008) 1998–2005.
[24] M. Panizza, G. Cerisola, Direct and mediated anodic oxidation of organic pollutants, Chem. Rev. 109 (2009) 6541–6569.
[25] C. Flox, C. Arias, E. Brillas, A. Savall, K. Groenen-Serrano, Electrochemical incineration of cresols: a comparative study between $PbO_2$ and boron-doped diamond anodes, Chemosphere 74 (2009) 1340–1347.
[26] M. Hamza, R. Abdelhedi, E. Brillas, I. Sirés, Comparative electrochemical degradation of the triphenylmethane dye methyl violet with boron-doped diamond and Pt anodes, J. Electroanal. Chem. 627 (2009) 41–50.
[27] E. Brillas, S. Garcia-Segura, M. Skoumal, C. Arias, Electrochemical incineration of diclofenac in neutral aqueous medium by anodic oxidation using Pt and boron-doped diamond anodes, Chemosphere 79 (2010) 605–612.
[28] A. Safarzadeh-Amiri, J.R. Bolton, S.R. Cater, Ferrioxalate-mediated solar degradation of organic contaminants in water, Solar Energy 56 (1996) 439–443.
[29] J.M. Chacon, M.T. Leal, M. Sanchez, E.R. Bandala, Solar photocatalytic degradation of azo-dyes by photo-Fenton process, Dyes Pigments 69 (2006) 144–150.
[30] M.F. Coughlin, B.K. Kinkle, P.L. Bishop, High performance degradation of azo dye Acid Orange 7 and sulfanilic acid in a laboratory scale reactor after seeding with cultured bacterial strains, Water Res. 37 (2003) 2757–2763.
[31] N. Yemashova, A. Telegina, I. Kotova, A. Netrusov, S. Kalyuzhnyi, Decolorization and partial degradation of selected azo dyes by methanogenic sludge, Appl. Biochem. Biotechnol. 119 (2004) 31–40.
[32] Y.Q. Wang, J.S. Zhang, J.T. Zhou, Z.P. Zhang, Biodegradation of 4-aminobenzenesulfonate by a novel *Pannonibacter* sp. W1 isolated from activated sludge, J. Hazard. Mater. 169 (2009) 1163–1167.
[33] G.H. Ming, S. Shafinaz, I. Zaharah, Y. Adibah, Biodegradation of 4-aminobenzenesulfonate by *Ralstonia* sp. PBA and *Hydrogenophaga* sp. PBC isolated from textile wastewater treatment plant, Chemosphere 82 (2011) 507–513.
[34] S. Gul, O. Serindag, H. Boztepe, Effects of ozonation on COD elimination of substituted aromatic compounds in aqueous solution, Turk. J. Chem. 23 (1999) 21–26.
[35] V. Santos, J. Diogo, M.J.A. Pacheco, L. Ciríaco, A. Morão, A. Lopes, Electrochemical degradation of sulfonated amines on Si/BDD electrodes, Chemosphere 79 (2010) 637–645.
[36] L. Hu, P.M. Flanders, P.L. Miller, T.J. Strathmann, Oxidation of sulfamethoxazole and related antimicrobial agents by $TiO_2$ photocatalysis, Water Res. 41 (2007) 2621–2626.
[37] D. Marciocha, J. Kalka, J. Turek-Szytow, J. Wiszniowski, J. Surmacz-Gorska, Oxidation of sulfamethoxazole by UVA radiation and modified Fenton reagent: toxicity and biodegradability of by-products, Water Sci. Technol. 60 (2009) 2555–2562.
[38] C. Carvalho, A. Fernandes, A. Lopes, H. Pinheiro, I. Gonçalves, Electrochemical degradation applied to the metabolites of Acid Orange 7 anaerobic biotreatment, Chemosphere 67 (2007) 1316–1324.
[39] R.H. Myers, D.C. Montgomery, Response Surface Methodology, Wiley, New York, 2002.
[40] M.A. Bezerra, R.E. Santelli, E.P. Oliveira, L.S. Villar, L.A. Escaleira, Response surface methodology (RSM) as a tool for optimization in analytical chemistry, Talanta 76 (2008) 965–977.
[41] I. Grcic, D. Vujevic, J. Sepcic, N. Koprivanac, Minimization of organic content in simulated industrial wastewater by Fenton type processes: a case study, J. Hazard. Mater. 170 (2009) 954–961.
[42] O. Rozas, D. Contreras, M.A. Mondaca, M. Pérez-Moya, H.D. Mansilla, Experimental design of Fenton and photo-Fenton reactions for the treatment of ampicillin solutions, J. Hazard. Mater. 177 (2010) 1025–1030.

[43] F. Ay, E.C. Catalkaya, F. Kargi, A statistical experiment design approach for advanced oxidation of Direct Red azo-dye by photo-Fenton treatment, J. Hazard. Mater. 162 (2009) 230–236.
[44] A. Zapata, I. Oller, E. Bizani, J.A. Sánchez-Pérez, M.I. Maldonado, S. Malato, Evaluation of operational parameters involved in solar photo-Fenton degradation of a commercial pesticide mixture, Catal. Today 144 (2009) 94–99.
[45] J.M. Monteagudo, A. Duran, I. San Martin, M. Aguirre, Catalytic degradation of Orange II in a ferrioxalate-assisted photo-Fenton process using a combined UV-A/C–solar pilot–plant system, Appl. Catal. B: Environ. 95 (2010) 120–129.
[46] J. Virkutyte, E. Rokhina, V. Jegatheesan, Optimisation of electro-Fenton denitrification of a model wastewater using a response surface methodology, Bioresour. Technol. 101 (2010) 1440–1446.
[47] S. Mohajeri, H.A. Aziz, M.H. Isa, M.A. Zahed, M.N. Adlan, Statistical optimization of process parameters for landfill leachate treatment using electro-Fenton technique, J. Hazard. Mater. 176 (2010) 749–758.
[48] M. Skoumal, C. Arias, P.L. Cabot, F. Centellas, J.A. Garrido, R.M. Rodríguez, E. Brillas, Mineralization of the biocide chloroxylenol by electrochemical advanced oxidation processes, Chemosphere 71 (2008) 1718–1729.
[49] G.E.P. Box, N.R. Draper, Empirical Model-Building and Response Surfaces, Wiley, New York, 1987.
[50] R.E. Bruns, I.S. Scarminio, B.B. Neto, Statistical Design-Chemometrics, Elsevier, Amsterdam, 2006.
[51] J. Feng, X. Hu, P.L. Yue, H.Y. Zhu, G.Q. Lu, Degradation of azo-dye Orange II by a photoassisted Fenton reaction using a novel composite of iron oxide and silicate nanoparticles as catalyst, Ind. Eng. Chem. Res. 42 (2003) 2058–2066.
[52] M.M. Ghoneim, H.S. El-Desoky, N.M. Zidan, Electro-Fenton oxidation of Sunset Yellow FCF azo-dye in aqueous solutions, Desalination 274 (2011) 22–30.
[53] S. Trabelsi, N. Oturan, N. Bellakhar, M.A. Oturan, Application of Doehlert matrix to determine the optimal conditions for landfill leachate treatment by electro-Fenton process, J. Mater. Environ. Sci. 3 (2012) 426–433.